

Creep degradation mechanism by water-rock interaction in the red-layer soft rock

H.F. Deng^{1,2,3} · M.L. Zhou^{2,3} · J.L. Li^{2,3} · X.S. Sun^{2,3} · Y.L. Huang¹

Received: 25 September 2015 / Accepted: 25 July 2016 / Published online: 18 August 2016
© Saudi Society for Geosciences 2016

Abstract Bank slope stability has become a great concern, while the impoundment of Three Gorges reservoir. The bank slope composed of red-layer soft rock has exhibited distinct deformation and failure. Therefore, a typical red-layer soft rock around Three Gorges reservoir area was selected to demonstrate the process of cyclic changes at the reservoir level and immersion-air-dry cyclic action of water-rock inside hydro-fluctuation belt. To meet the objective of this study, a series of creep tests were conducted on the rock specimens at different water-rock interaction stages. The following points were noticed based on the laboratory results: (1) the creep fracture strength and long-term strength of red-layer soft rock degraded significantly during the process of water-rock interaction. For the first three water-rock interaction circulations, the strength of red-layer soft rock degraded quickly and then gradually became stable. (2) During the creep test, the lateral expansion of red-layer soft rock increased significantly regarding to the number of cycles. (3) The creep curve includes three typical stages at failure stress level—primary (damped) stage, secondary (steady-state) stage, and tertiary (nonlinear accelerated) stage. As the number of cycles increased, the percentage of secondary stage diminished gradually.

However, the tertiary stage showed a gradual increment, since the plasticity of the specimens was strengthened by water-rock interaction. (4) The shear failure characteristics of the specimens became highly considerable during the process of water-rock interaction, and there have been a gradual increment of shear rupture zone. (5) The SEM results showed that the specimen microstructure changed its state from dense to loose and porous. The findings of this research provide a good basis for long-term stability analysis of bank slope.

Keywords Bank slope, Red-layer soft rock, Water-rock interaction, Creep, Long-term strength, Failure characteristics

Introduction

Following the completion of the Three Gorges hydropower project, the reservoir level has been fluctuating yearly by 145 m from its flood control water level and 175 m from its electricity generation water level. The hydro-fluctuation belt will have 30-m height. Gradually, a number of bank slopes experienced larger deformation and they have exhibited failure since June 2003. Successive and considerable amount of water level fluctuations signify the problems of bank slope stability. The deformation and failure of slopes made of red-layer soft rocks are especially problematic. According to incomplete statistics, about 69 % (Chai et al. 2009; Li et al. 2004; Jian et al. 2005), of landslide disasters in the region, managed and monitored during the second and third governance phases in the vicinity of Three Gorges reservoir, consisted of red layers. Such as Gangtie landslide in Chongqing, the four major landslide groups in Wanzhou, Jipazi landslide in Yunyang, and Qianjiangping landslide in Yichang etc. Qianjiangping landslide occurred in 2003, after 33 days

✉ H.F. Deng
dhf8010@ctgu.edu.cn

¹ State Key Laboratory of Simulation and Regulation of Water Cycle in River Basin, China Institute of Water Resources and Hydro-power Research, Beijing, China

² Collaborative Innovation Center for Geo-Hazards and Eco-Environment in Three Gorges Area, Hubei Province, Yichang, Hubei, China

³ Key Laboratory of Geological Hazards on Three Gorges Reservoir Area (China Three Gorges University), Ministry of Education, Yichang 443002, Hubei, China



Fig. 1 Typical rock samples

of the first water storage (i.e., 135-m height of water in the Three Gorges reservoir area). It was the first large wading landslide following the initial water storage. Studies have shown that the deformation and failure of Bank slopes were often closely related to rheological mechanical properties of red-layer soft rock under water-rock interaction (Chai et al. 2009; Li et al. 2004; Jian et al. 2005; Wang et al. 1996).

As a special kind of rock, soft rock is a complex rock medium that shows significant plastic deformation under specific environment. This kind of rock is widely available in all kinds of constructions: slope engineering, water resources, and hydropower engineering and always play a governing role in the stability of slopes, dam foundations, and underground caverns (He et al. 2002; Liu and Lin 2001). Recently, attempts have done by different investigators to study the mechanical characteristics of soft rock. The water-rock interaction of soft rock has been studied

based on microscopic structure, ion concentration, and variations in mechanical properties. It was found that the physical and mechanical properties of soft rock and the ionic concentration of water solution changed dramatically within the first 3 months and stabilized gradually (Zhou et al. 2003; 2004; 2005; 2010). Rheological tests have been conducted on the various types of rocks such as clay rock, soft rock, halite, soft interlayer, mudstone (Gascbarbier et al. 2004; Wang et al. 2007; Xu et al. 2006; Yang et al. 2007), and carbonaceous shale (Shen et al. 2010). The above three studies showed that long-term strength of saturated rock reduced, while the creep velocity and deformation values alarmingly increased under dry and saturated conditions. According to Jian Liu (Lu et al. 2008), creep is more remarkable in saturated sandstones than dry sandstones. The creep properties of sandstone with different flow solution were more remarkable than dry and saturated sandstone. A series of direct shear tests were conducted to examine the effect of water saturation on the mechanical properties of clay-infilled discontinuities (Pellet et al. 2013), results showed that both angle of friction and cohesion decreased while the discontinuity was saturated, and the shear strength of the discontinuity exhibited about 50 % reduction from its original value. Triaxial deformation experiments were performed on a porous limestone saturated with water (Brantut et al. 2014), this study revealed that only small strains were built up during the occurrence of brittle creep failure, and the damage increased little with strain. A constitutive model was proposed to describe the time-dependent

Fig. 2 X-ray diffraction spectrum of rock samples

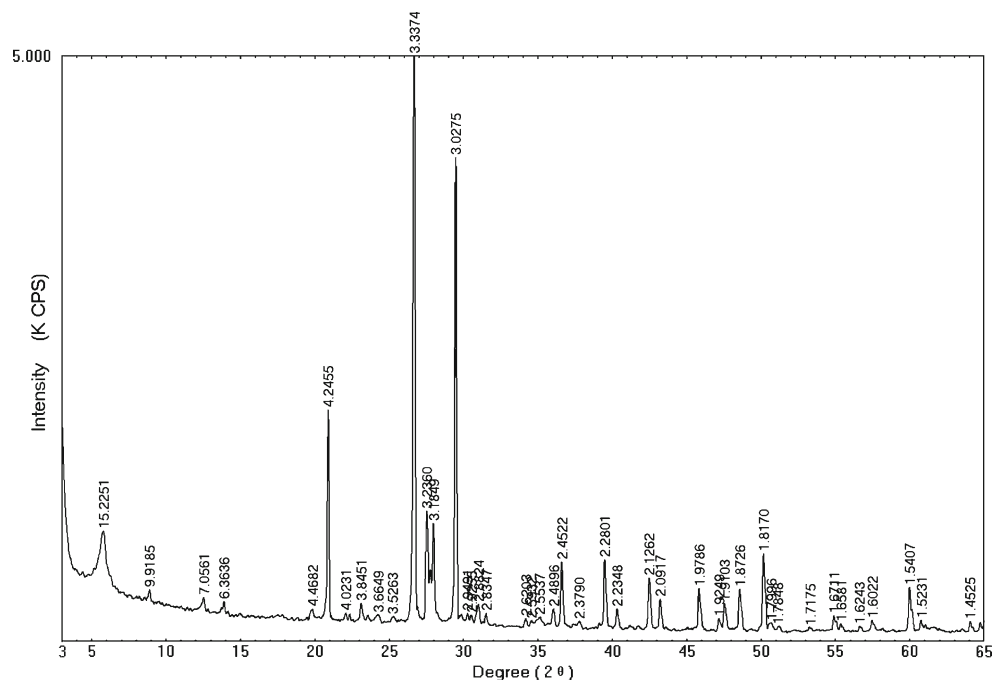
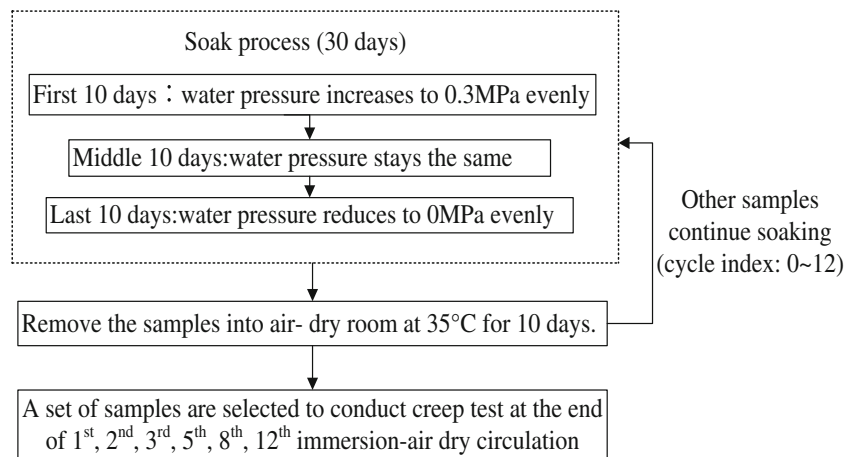


Fig. 3 Flow chart of immersion-air-dry circulation

behavior and wetting deterioration of sandstone (Weng 2014). The effect of fluid injection on the mechanical behavior of the weakly consolidated Sherwood sandstone was studied using laboratory experiments (David et al. 2015), the observations show that water injection triggered mechanical instability (macroscopic failure) within half an hour, and the mechanical instability was probably linked to the loss of cohesion in the water-invaded region.

From these studies, the following conclusions can be arrived. The water-rock interaction would weaken the physical and mechanical properties of soft rock. The rheological behavior of soft rock was considerable, and the long-term strength was decreased significantly under saturated state. During the previous studies, either dry or saturated conditions were considered and the effect of long-term water-rock interaction of the bank slope on the creep mechanical properties of soft rock was not studied well. Therefore, a typical red-layer soft rock in Three Gorges reservoir area was selected to meet the objectives of this study. A series of water-rock interaction tests were carried out to simulate the fluctuations of water level in

the vicinity of hydro-fluctuation belt. Creep tests were conducted under different water-rock interaction stages to study the deteriorating action and weakening mechanisms of the red-layer soft rock.

Test scheme

Sample preparation

A typical bank slope comprised of red-layer soft rock in Three Gorges reservoir area was selected, and samples were taken from the hydro-fluctuation belt. The test specimens were prepared based on the specification requirements ($\Phi 50\text{mm} \times 100\text{mm}$) as shown in Fig. 1. Besides, samples with obvious defects were rejected. *P*-wave velocity and rebound value were scrutinized to eliminate samples with extreme outliers (Deng et al. 2011).

X-ray diffraction was employed to identify mineral contents of the specimens; the XRD spectrum is shown in Fig. 2. The identification test showed that the rock class was argillaceous siltstone, and the mineral contents (mass fraction) were as follows: smectite 15 %, chlorite 5 %, illite 5 %, quartz 33 %, feldspar 15 %, calcite 25 %, and dolomite 2 %.

Water-rock interaction testing program

The aim of this paper was to simulate reservoir fluctuation and immersion-air-dry circulation (i.e., real condition of bank slope). The experiment procedure is clearly shown in Fig. 3, rock samples were placed inside a rock dissolution apparatus, and every immersion stages took 30 days; during the first 10 days, the rise in the reservoir water level was simulated by evenly increasing the water pressure to 0.3 MPa. Since the studied reservoir water level has been fluctuating from 145 to 175 m, a 0.3 MPa pressure was chosen as a proxy of water pressure. The relative stability period of the reservoir water

**Fig. 4** YRK-1 rock dissolution apparatus

Table 1 Creep test stress loading scheme

Sample number	Water-rock interaction cycle	Initial axial stress σ_1 /MPa	Axial stress increment/MPa						Axial failure stress σ_1 /MPa
			First step	Second step	Third step	Fourth step	Fifth step	Sixth step	
C16-1	0	20.00	2.50	2.50	1.25	1.25	1.25	–	28.75
C20-10	1	15.00	1.50	1.50	–	–	–	–	18.00
C20-5	2	10.00	1.50	1.50	1.50	–	–	–	14.50
C17-6	3	10.00	1.50	1.50	–	–	–	–	13.00
C14-9	5	6.00	1.00	1.00	1.00	1.00	1.00	1.00	12.00
C16-5	8	6.00	1.00	1.00	1.00	1.00	1.00	–	11.00
C17-9	12	6.00	1.00	1.00	1.00	1.00	–	–	10.00

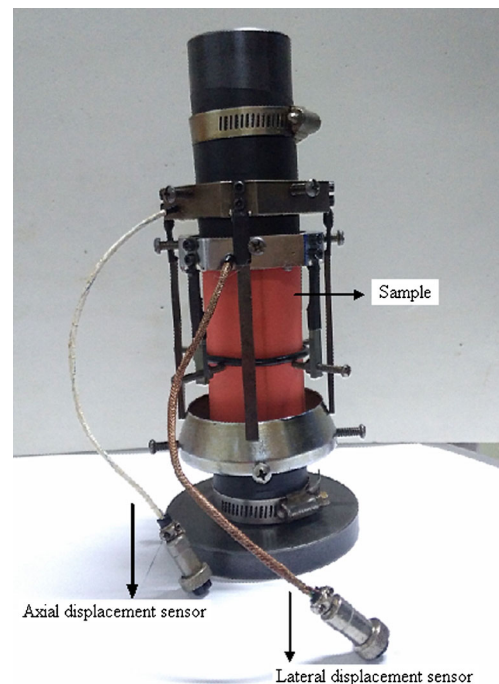
was simulated during the next 10 days. Finally, the pressure was reduced uniformly to 0 MPa during the last 10 days to simulate the drop in the reservoir water level. Consequently, soaked samples were air-dried at 35 °C room temperature (since, the temperature of the studied area during the impoundment season was around 35 °C) for 10 days to replicate the natural air-dry process of the bank slope following the reduction in the water level. A set of samples were chosen from the air-dried ones to conduct creep test at the end of the first, second, third, fifth, eighth, 12th immersion-air-dry circulation, and the other samples were replaced to the rock dissolution apparatus to keep the immersion-air-dry circulation. A total of 12 cycles were executed during the experiment.

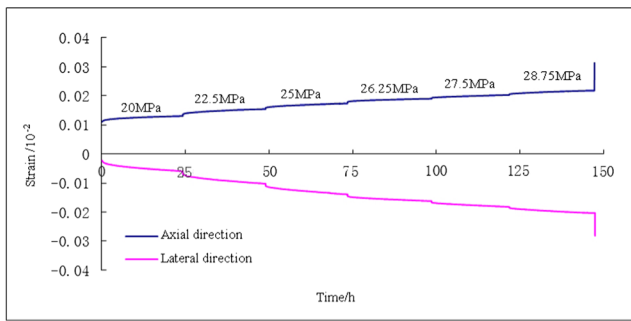
The dissolution apparatus is shown in Fig. 4. It was used to soak rocks during water-rock interaction test. The fluctuations of water pressure can be well simulated by the process of soaking.

**Fig. 5** RLW-2000 rock creep testing machine

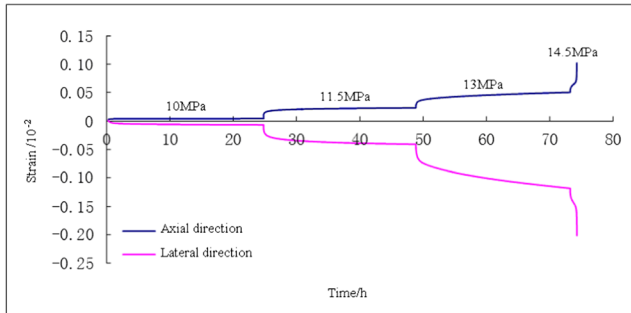
Creep testing program

As previously discussed, a group of rock specimens was chosen to conduct creep test at the end of each cycle. For the sake of comparison, creep tests were conducted on one group of saturated rock specimens, before water-rock interaction tests were being executed. The employed confining pressure was 5 MPa, axial stress was applied using 3 to 6 steps, and each step took about 24 h. The next loading step was done while the strain increment <0.001 mm/h and the loading were continued until the failure emerged. About 60 % of triaxial test ultimate strength was taken as the initial axial stress for the creep test. Moreover, initial axial stress and its increment were adjusted for each creep test (as the strength of rock specimens plunged during the process of water-rock

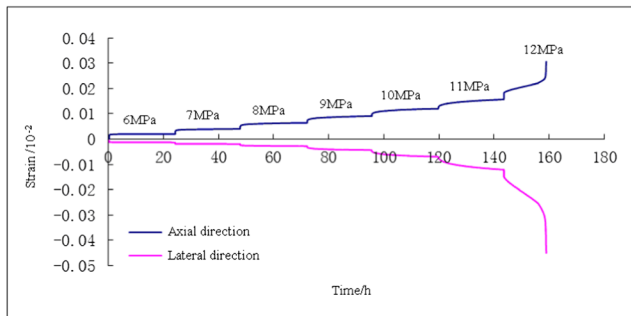
**Fig. 6** The sample ready for test



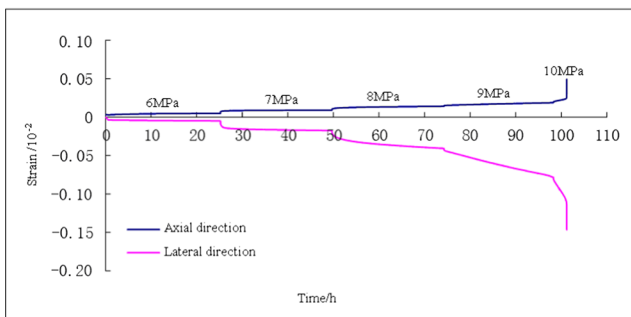
(a) C16-1 creep curves at confining pressure 5MPa (0 cycle)



(b) C20-5 creep curves at 5MPa confining pressure (2 cycles)



(c) C14-9 creep curves at 5MPa confining pressure (5 cycles)



(d) C17-9 creep curves at 5MPa confining pressure (12 cycles)

Fig. 7 Axial and lateral creep curves for the red-layer soft rock under different water-rock interaction cycles. **a** C16-1 creep curves at confining pressure 5 MPa (0 cycle). **c** C20-5 creep curves at 5 MPa confining pressure (2 cycles). **e** C14-9 creep curves at 5 MPa confining pressure (5 cycles). **g** C17-9 creep curves at 5 MPa confining pressure (12 cycles)

interaction). The applied axial stress during the test is shown in Table 1.

The creep tests were conducted using RLW-2000 rock creep test machine, as shown in Fig. 5. The sample is sealed with heat shrinkable tube, and the axial and lateral strains are collected by displacement sensors, as shown in Fig. 6. The testing temperature was set to 20 ± 2 °C.

Results and discussions

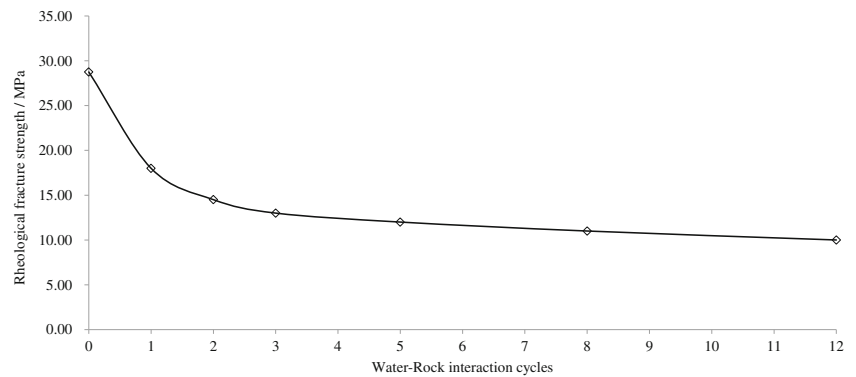
Axial and lateral creep deformation

Figure 7 shows the axial and lateral strain of initially saturated rock specimens under different water-rock interaction cycles. The curves for various stress levels were obtained by using superposition principle. The applied pressures were displayed on the curve. Similarly, the degradation in fracture strength of red-layer soft rock under water-rock interaction cycles is shown Fig. 8.

After careful investigation of Fig. 7 and Fig. 8, the following conclusions were made:

- (1) Red-layer soft rock showed considerable creep deformation in all stress levels. Axial and lateral deformation incorporated instantaneous and creep deformations. Each step of creep deformation included primary stage and secondary stage under low axial stress level. The smaller deviatoric stress had the smaller primary creep deformation and time as well. The duration and slope of primary stage curve increased, while the deviatoric stress increased. The creep deformation curve had tertiary stage at the failure stress level. The duration of this stage was short. However, samples were quickly broken due to large deformation.
- (2) The comparative study of creep curves for rock samples under different water-rock interaction cycles revealed that the strength of the samples decreased gradually, while the water-rock interaction cycles increased. The failure strength of soft rock decreased by 37, 55, and 62 % from its initial strength, during the first, the third, and the eighth water-rock interaction cycles, respectively. Relatively, the degradation rate of soft rock strength was fast during the first three cycles and then gradually became stable.
- (3) Instantaneous and creep deformations rose gradually, when water-rock interaction cycles increased (by keeping constant axial stress increment). The rheological properties of the samples were considerable and conformed to the creep deformation characteristics of actual bank slope affected by the water-rock interaction.

Fig. 8 Fracture strength degradation curve for the red-layer soft rock under different water-rock interaction cycles



- (4) When the water-rock interaction increased, the lateral creep deformation was higher than the axial creep deformation under same axial stress. Effect of lateral dilation was more pronounced, while the applied axial stress moved towards the failure stress level.

Tertiary creep stage

Figure 9 shows the tertiary stage of axial and lateral creep velocity at the failure stress level for the red-layer soft rock specimens under different water-rock interaction cycles.

The following important points can be noticed from Fig. 9:

- (1) Observations of rock samples under different water-rock interaction cycles at the failure stress level were basically the same. All of the creep curves exhibited three typical stages—primary (damped), secondary (steady-state), and tertiary (nonlinear accelerated) stages. The deformation at each stage was significant. Generally, both primary and tertiary stages took short period of time. In contrast, secondary stage spent long period of time.
- (2) During the early stage of water-rock interaction, the average creep velocity at the secondary stage was relatively low. While, the average creep velocity at the tertiary stage was high and the samples were broken suddenly. As water-rock interaction cycles increased, the average creep velocity at the secondary stage increased gradually. Nonetheless, the creep velocity at the tertiary stage decreased smoothly. The percentage of time taken by the tertiary stage increased steadily. However, the fragility of the rock has reduced slowly.
- (3) The time spent for each stage at the failure stress level under different water-rock interaction cycles is shown in Table 2. Considering failure stress level at the secondary stage, the average creep velocity in the lateral direction

was higher than that in the axial direction. The discrepancy became noticeable while water-rock interaction cycles increased. For example, the average creep velocity ratio of lateral to axial were 1.71, 2.39, and 4.26 during the first water-rock interaction cycle, the third water-rock interaction cycle, and the twelfth water-rock interaction cycle, respectively. The result revealed that the rock properties became softer and more likely produced lateral expansion deformation during the process of water-rock interaction.

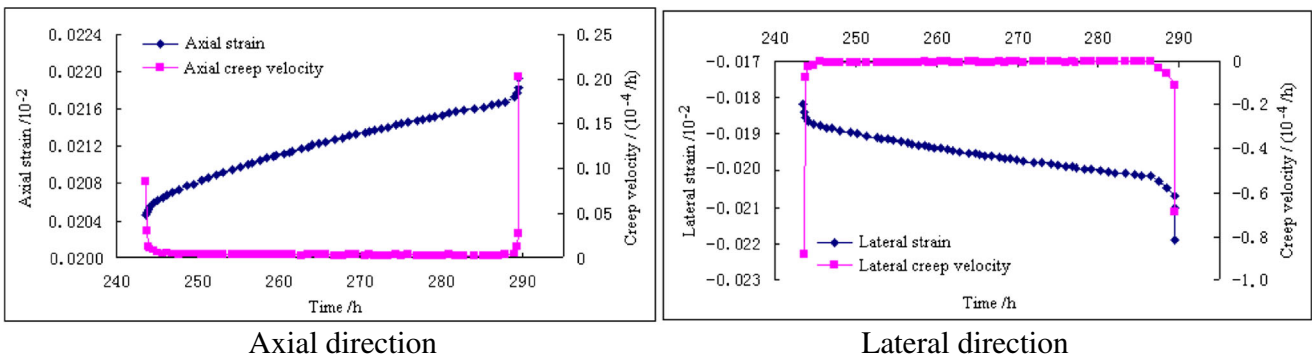
Long-term strength

The long-term strength of a rock is a strength index of a rock mass obtained by considering aging characteristics. Obviously, it will be lower than the conventional instantaneous intensity. The long-term strength of red-layer soft rock was determined by using stress-strain isochronous curves, according to *Specifications for rock tests in water conservancy and hydroelectric engineering (SL264-2001)*. The ratio of long-term strength and creep failure strength was defined as long-term strength ratio, as shown in Table 3.

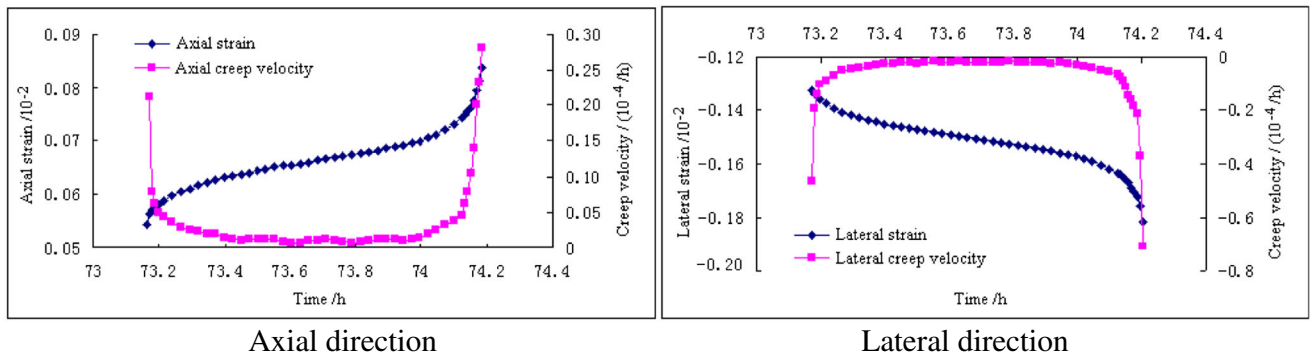
One can understand the following key points from Table 3.

- (1) The long-term strength of soft rock reduced gradually during the process of water-rock interaction, compared to the initially saturated one. Moreover, the long-term

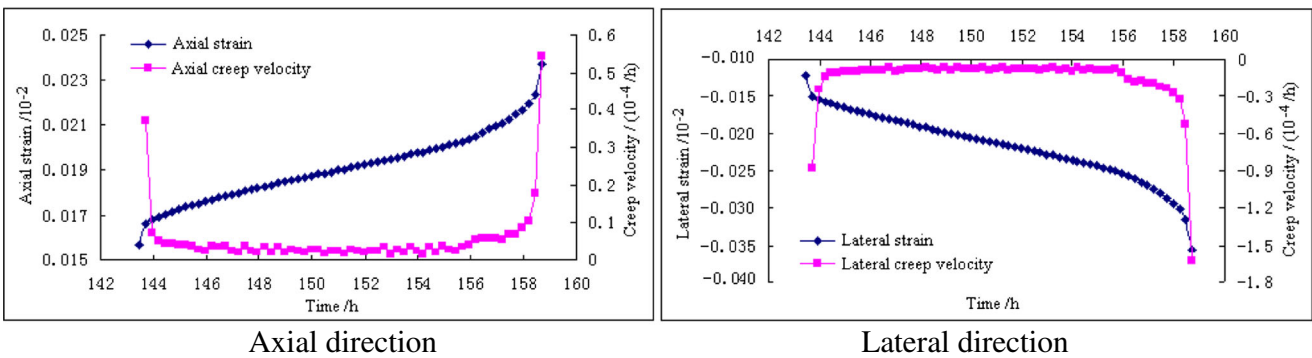
Fig. 9 Axial and lateral creep velocity curves of rock samples under different water-rock interaction cycles at the failure stress level. **a** C16-1 the relationship between strain, creep velocity, and time at the failure stress level (0 cycle). **c** C20-5 the relationship between strain, creep velocity, and time at the failure stress level (2 cycles). **g** C14-9 the relationship between strain, creep velocity, and time at the failure stress level (5 cycles). **e** C17-9 the relationship between strain, creep velocity, and time at the failure stress level (12 cycles)



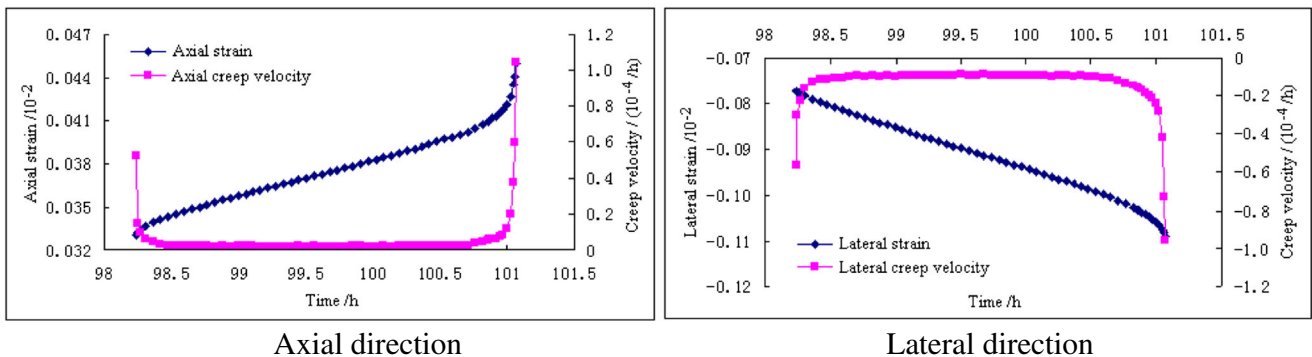
(a) C16-1 the relationship between strain, creep velocity and time at the failure stress level (0 cycle)



(b) C20-5 the relationship between strain, creep velocity and time at the failure stress level (2 cycles)



(c) C14-9 the relationship between strain, creep velocity and time at the failure stress level (5 cycles)



(d) C17-9 the relationship between strain, creep velocity and time at the failure stress level (12 cycles)

Table 2 Duration of different creep stage for different rock samples at the failure stress level

Sample number	Water-rock interaction cycle	Secondary stage				Proportion of tertiary stage in total duration (%)
		Proportion in total duration (%)	Average creep velocity (10^{-4} /h)		Creep velocity ratio for lateral to axial direction	
			Axial direction	Lateral direction		
C16-1	0	74.09	0.0028	0.0034	1.21	9.33
C20-10	1	69.08	0.025	0.0428	1.71	13.89
C20-5	2	65.55	0.029	0.0624	2.15	17.65
C17-6	3	64.81	0.034	0.0812	2.39	20.37
C14-9	5	63.93	0.037	0.096	2.59	22.95
C16-5	8	62.84	0.033	0.114	3.45	22.31
C17-9	12	62.42	0.034	0.1448	4.26	22.94

strength of soft rock dropped by 40, 60, and 68 % following one water-rock interaction cycle, three water-rock interaction cycles, and eight water-rock interaction cycles, respectively. The change in long-term strength was consistent with the degradation of creep failure strength.

- (2) The long-term strength of the samples was about 70–87 % of the creep failure strength. In the mean time, the long-term strength ratio plunged as water-rock interaction cycles increased, suggesting that water-rock interaction resulted an earlier occurrence of yield and failure of red-layer soft rock.

Failure characteristics of rock samples

Figure 10 shows crack patterns of the rock specimens under different water-rock interaction cycles.

As it can be seen from Fig. 9, the failure patterns of samples were not unique under different water-rock interaction cycles:

- (1) Generally, the failure patterns of sandstone samples suggested that the rock samples had obvious shear failure characteristics under different water-rock interaction cycles. Most of the principal shear failure planes were extended from one end to another end of the samples. One or two interconnected shear planes took place when the samples failed, and the lateral deformation occurred on the samples.
- (2) Comparatively, some tension cracks were developed during the early stage of water-rock interaction and yielded severe cracks. Later on, the governing shear surfaces of the failed samples became considerable. Besides, further secondary cracks appeared on both sides of the shear rupture zone. The ballooning phenomenon was noticeable by its “big belly” characteristic.
- (3) Noticeable faults were emerged on both sides of the shearing surface (since, the failed samples exhibited considerable amount of shear deformation).

Microstructure characteristics of red-layer soft rock under water-rock interaction

Scanning electron microscopy (SEM) analysis was carried out on the samples under different water-rock interaction cycles. Results are shown in Fig. 11.

The following valuable points were made based on SEM micrographs.

- (1) In the beginning, saturated samples had angular mineral particles, comprised of irregular polygon. Additionally, the particles made good contact with each other and the contact surface was flat and smooth, characterized by clear boundaries and tiny cracks on it.

Table 3 Creep long-term strength of rock samples during the process of water-rock interaction

Water-rock interaction cycle	Failure stress/MPa	Long-term strength/MPa	Long-term strength ratio (%)
0	28.75	25	86.96
1	18	15	83.33
2	14.5	11.5	79.31
3	13	10	76.92
5	13	10	76.92
8	11	8	72.73
12	10	7	70.00

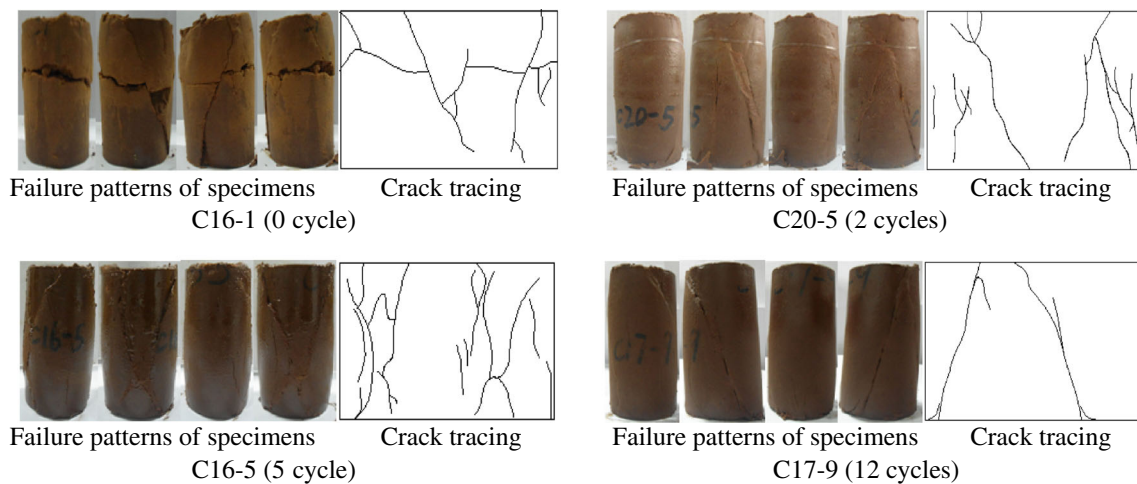


Fig. 10 Crack patterns of typical rock specimens

- (2) After the first water-rock interaction cycle, boundaries of particles became fuzzy, tiny pores and cracks developed, and partial protuberance on the surface of the particles gradually converted into round shape during the water-rock interaction.
- (3) The surface of mineral particles was no longer flat following the second water-rock interaction cycle. In the mean time, edges and corners at the convex position were gradually converted into sleek and small corrosion pits developed by water-rock interactions emerged on the surface of mineral particles. Moreover, micro cracks and pores developed gradually.
- (4) Following the third water-rock interaction cycle, the contact between mineral particles has changed from surface-surface to edge-angular. Similarly, micropores have emerged and clear cracks noticed on some large particles. In the mean time, small particles rose significantly and the structure became porous and loose in time.
- (5) To come to the fifth water-rock interaction cycle, loose particles slightly fragmented into small particles and congregated around the large particles. Pores and cracks between the mineral particles became clearer, and the boundaries seemed sleeker. Meanwhile, small particles got smaller and smoother and the structure turned out into a more loose and porous state.
- (6) More globular particles adhered to the surface of mineral particles. Likewise, large particles disintegrated into small particles. Pores and cracks between particles have been filled during the eighth water-rock interaction cycle.
- (7) Considering the last water-rock interaction cycle, the structure has changed its state from dense to loose and porous state. The contacts between the particles were predominantly edge-edge and edge-corner connections.

Generally, micro cracks and pores of rock samples were developed gradually, during the process of water-rock interactions. Boundaries of large particles appeared to be sleeker and more remarkable. Pores and cracks between the mineral particles became clearer. In the mean time, small particles got smaller and smoother and the structure turned out in to a more loose and porous state.

Mechanical properties degradation of red-layer soft rock under water-rock interaction

Rocks have a lot of micro defects. Some structures such as joint gaps, cracks distribution zone, and plastic zone at the crack tip were the regions that could be actively affected by the water-rock interaction, physically and chemically with significant dispersion. Impact of water-rock interaction on the rock mass is a complex phenomenon (Liu et al. 2009; Deng et al. 2013), and the change in microstructure yielded macroscopic degradation of mechanical parameters (Liu et al. 2008). It was important to analyze the effects of water pressure fluctuation and immersion–air-dry cycle on the degradation mechanisms of the rock, as those conditions considered during the water-rock interaction test.

- (1) During the process of increasing water pressure, the reservoir water infiltrated inside the rock samples. On the one hand dissolution, corrosion and other chemical reactions occurred in the mineral particles. On the other hand, dissolution and chemical migration occurred at the contact surfaces or cemented between mineral particles. Consequently, mineral compositions and microstructures of the rock have changed (Chen 2006). The effects of those two aspects have been pronounced, since the red-layer soft rock comprised of many minerals that can easily expand inside the water. Under the water pressure, the crack was likely propagated by the stress concentrated at

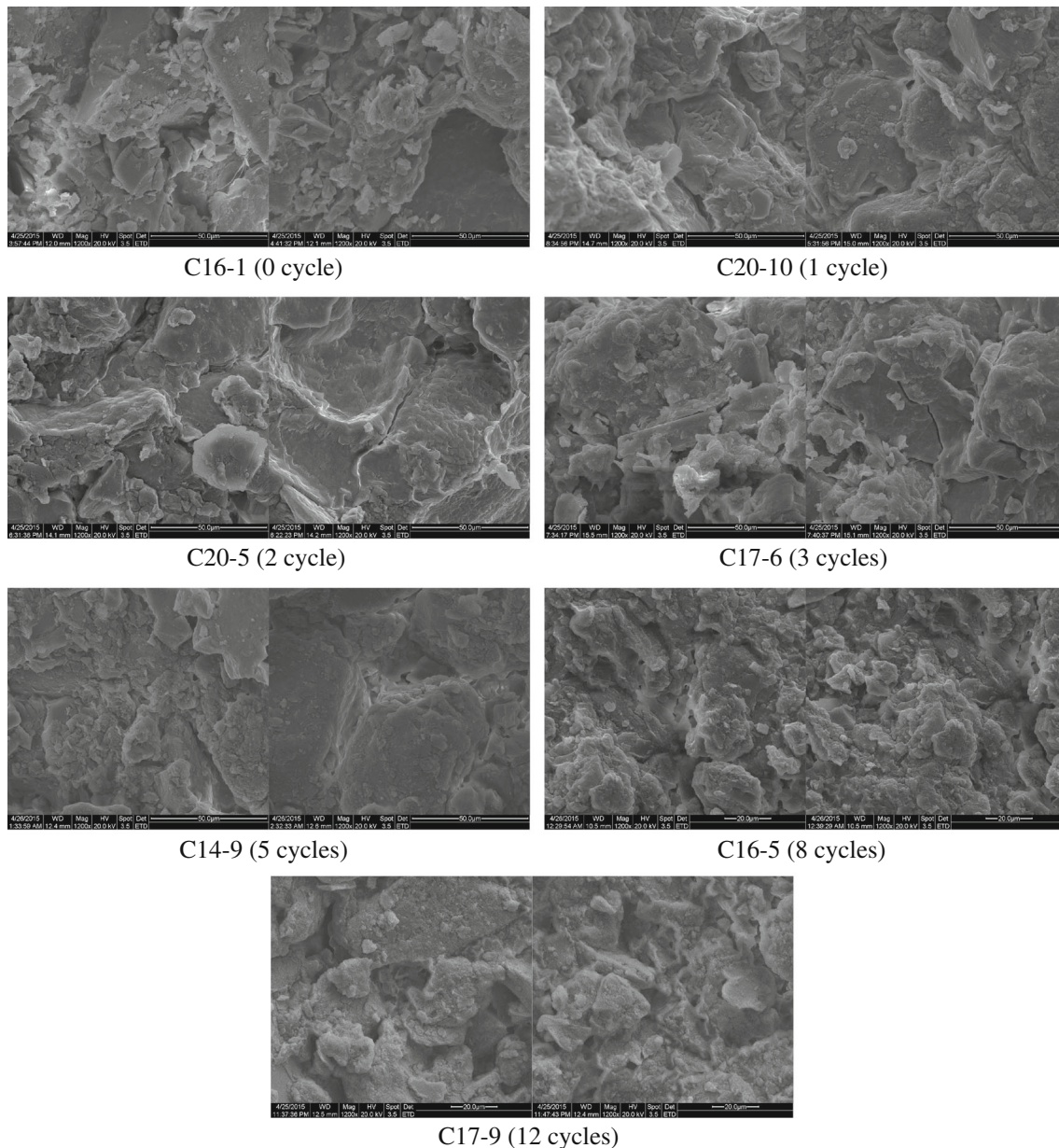


Fig. 11 Microstructure changes on the specimens during the process of water-rock interaction (1200 \times)

the endpoints of the crack (Tang et al. 2003). It was favorable for the formation of infiltration channels, seepage, and exosmoses of water molecules within the rock samples. It has increased surfaces for the water-rock reaction (physical and chemical). The reactions between aqueous solution and rock minerals were accelerated, which increased the change in microstructure and promoted the extension and coalescence of gaps and cracks.

(2) The water molecule exosmoses during the process of air-drying and water pressure decline. Mineral particles and chemical substance exosmoses along the cracks, pores, and contact surface between particles developed new secondary pores and cracks, which

provided more new reaction surface for the next water-rock physical and chemical reactions. Note that both mineral particles and chemical substances were developed by the water-rock physical and chemical interactions. Microstructure characteristic change of the samples in different water-rock interaction cycles is shown in the SEM pictures above.

(3) The process of immersion-air-dry circulation could not only change the dissolution pattern and intensity during the water-rock interaction but also changed the dissolution-precipitation direction (Huang et al. 2010) that would intensify the water-rock interaction and develop new physical and chemical damages on



Fig. 12 Typical failures of red-layer soft rock in the vicinity of hydro-fluctuation belt in Three Gorges reservoir area (July 2013)

the rock, resulting in a gradual drop in the rock strength.

In general, the process of water-rock interaction under water pressure fluctuation would develop a built up damage. The rock mineral structure has changed from dense to loose and porous at the micro level and yielded degradation of mechanical properties at the macro level.

Water-rock interaction gradually became balanced with the stabilization of soaking solution environment (Zhou et al. 2010). Previous studies showed that during the preliminary tests, rock strength deteriorated quickly. However, after 3 cycles of immersion-air-dry circulations, the water-rock interaction and strength deterioration rate of the rock samples decelerated.

The built up damages on the bank slopes, due to successive fluctuations in the reservoir water level, will not be noticed at a time. But after repeated actions, the damage may build up and it will result to slope instability. Statistics showed that many bank slope instability did not occur during the initial time of water storage but after several rise and fall cycles of reservoir water. This can be proven from the real failure phenomena of the rock bank slope. Figure 12 shows a typical failure of rocks in the vicinity of hydro-fluctuation belt bank slopes.

The impoundment of the reservoir has started since 2008 and stored water up to 172.8 m. Figure 12 shows that few floras have grown in the vicinity of the hydro-fluctuation belt (145~175 m). The cracks and fractures have developed with large openings. Stratified disintegration and fragmentation have occurred on the rock mass. This destruction revealed that the red-layer soft rock has been significantly affected by repeatedly fluctuating reservoir water.

Conclusions

The following conclusions were made based on the findings of this paper:

- (1) During the process of water-rock interaction, there has been deterioration in the creep fracture and the long-term strengths of the red-layer soft rock. Initially, the extent of deterioration was increased. However, it has shown reduction in time. For the first three water-rock interaction cycles, the degradation rate was relatively faster, the creep fracture and the long-term strengths were decreased by 55 and 60 %, respectively. Following three

water-rock interaction cycles, the strength of red-layer soft rock became stable.

- (2) The plasticity of red-layer soft rock improved, and the lateral expansion trend got noticeable, while the water-rock interaction cycles increased. In the mean time, the fragility of the rock has reduced slowly.
- (3) The shear failure characteristics of red-layer soft rock became noticeable during the process of water-rock interaction, and the influenced area of shear rupture zone rose steadily.
- (4) The process of water-rock interaction could result a built up damage. Moreover, the specimen structure changed from dense to loose and porous states, accompanied by micro fractures and pores. The change in microstructure resulted in degradation in the mechanical properties of soft rock.

Acknowledgments This work was supported by the Open Research Fund of State Key Laboratory of Simulation and Regulation of Water Cycle in River Basin (China Institute of Water Resources and Hydropower Research, Grant NO.IWHR-SKL-201316), the Master Thesis Fund of Civil and Architecture Institute of Three Gorges University (Grant No.2015PY11), and the National Natural Science Foundation of China (Grant No.51309141, 51439003).

References

- Brantut N, Heap MJ, Baud P, et al. (2014) Mechanisms of time-dependent deformation in porous limestone. *Journal of Geophysical Research-Solid Earth* 7:5444–5463
- Chen J (2006) Chemical water-rock interaction contribution to landslide preparation process. Dissertation, Kunming University of Science Technology
- Chai B, Yin K, Jian W, et al. (2009) Analysis of water-rock interaction characteristics and bank slope failure process of red-bed. *Journal of Central South University (Science and Technology)* 4:1092–1098
- David C, Dautriat J, Sarout J, et al. (2015) Mechanical instability induced by water weakening in laboratory fluid injection tests. *Journal of Geophysical Research-Solid Earth* 6:4171–4188
- Deng H, Li J, Deng C, et al. (2011) Analysis of sampling in rock mechanics test and compressive strength prediction methods. *Rock Soil Mech* 11:3399–3403
- Deng H, Yuan X, Wang L, et al. (2013) Experimental research on changes in the mechanical property law of reservoir bank sandstone under “immersion-air dry” circulation. *Environmental Engineering & Management Journal* 12(9):1785–1789
- Gasc-barbier M, Chanchole S, et al. (2004) Creep behavior of bure clayey rock. *Appl Clay Sci* 1(4):449–458
- Huang S, Gong Y, Huang K, Tong H (2010) The influence of burial history on carbonate dissolution and precipitation—a case study from fei xian guan formation of triassic NE Si chuan and ordovician carbonate of northern tarimbasin. *Dvancesin earth science* 4:381–390
- He M, Jing H, Sun X (2002) *Soft rock engineering mechanics*. Beijing.
- Jian W, Yin K, Ma C, et al. (2005) Characteristics of incompetent beds in Jurassic red clastic rocks in Wanzhou. *Rock Soil Mech* 6(901–905): 914
- Liu X, Fu Y, Wang Y (2009) Stability of reservoir bank slope under water-rock interaction. *Rock Soil Mech* 3:613–616,627
- Liu T, Lin T (2001) *Soft rock engineering design theory and construction practice*. Beijing
- Lu J, Li P, Qiao Y, Zhu J (2008) Experimental research on creep behavior and mechanism of sandstones with hydro-physico-chemical effects. *Chin J Rock Mech Eng* 12:2540–2550
- Li S, Li X, Zhang N, et al. (2004) Sedimentation characteristics of the jurassic sliding-prone stratum in the three gorges reservoir area and their influence on physical and mechanical properties of rock. *J Eng Geol* 4:385–389
- Pellet F, Keshavarz M, Boulon M (2013) Influence of humidity conditions on shear strength of clay rock discontinuities. *Eng Geol* 5:33–38
- Shen R, Liu C, Liu X (2010) Triaxial rheology characteristics and model of carbonaceous shale in pressure water. *Chinese Journal of Geotechnical Engineering* 32(7):1031–1034
- Tang L, Zhang P, Wang Y (2003) Propagation of the complex cracks in RocksII. Under Water Pressure and Chemical Damage *Acta scientiarum naturalium universitatis sunyatseni* 1:90–94
- Weng MC (2014) A generalized plasticity-based model for sandstone considering time-dependent behavior and wetting deterioration. *Rock Mech Rock Eng* 7:1197–1209
- Wang S, Ma F, Du Y (1996) On the rock-water interaction in reservoir areas and its geoenvironmental effect. *J Eng Geol* 3:1–9
- Wang Z, Yin K, Jian W (2007) Experimental research on creep of incompetent beds in Jurassic red clastic rocks in Wanzhou. *Rock and Soil Mechanics (Suppl)*:40–44
- Xu W, Zhou J, Yang S, et al (2006) Study on creep damage constitutive relation of greenschist specimen. *Chinese Journal of Rock Mechanics and Engineering (Suppl)*:3093–3097
- Yang S, Xu W, Yang S, et al. (2007) Investigation on shear rheological mechanical properties of shale in Longtan hydropower project. *Rock Soil Mech* 5:895–902
- Zhou C, Deng Y, Tan X (2003) Research on the variation regularities of microstructures in the testing of interaction between soft rocks and water. *Acat Scientiarum Naturalium Universitatis Sunyatsent* 4:98–102
- Zhou C, Deng Y, Tan X (2004) Testing study on variation regularities of solution components in saturation of soft rocks. *Chin J Rock Mech Eng* 22:3813–3817
- Zhou C, Deng Y, Tan X (2005) Experimental research on the softening of mechanical properties of saturated soft rocks and application. *Chin J Rock Mech Eng* 1:33–38
- Zhou C, Zhu F, Zhang L (2010) Research on saturation test and softening critical phenomena of soft rocks. *Rock Soil Mech* 6:1709–1715